THE ASTROPHYSICAL JOURNAL, 473:763–772, 1996 December 20

VARIABILITY OF *CGRO*/EGRET GAMMA-RAY SOURCES

M. A. MCLAUGHLIN,[1] J. R. MATTOX,[2,3] J. M. CORDES,[1] AND D. J. THOMPSON[4]

Received 1996 March 4; accepted 1996 July 15

ABSTRACT

We have developed a method for quantifying the flux variability of EGRET high-energy gamma-ray sources. We apply this method to all sources in the Second EGRET Catalog except for the one solar flare. Allowing for a small systematic uncertainty, the phase-averaged flux densities of the pulsars are consistent with being nonvariable. Many identified active galactic nuclei are variable, as expected, and it is likely that the apparent nonvariability of some identified active galactic nuclei results from decreased sensitivity to variability at low fluxes and low latitudes. Populations of both variable and nonvariable unidentified sources are found to be in excess at low Galactic latitudes. While low-flux, nonvariable, unidentified sources could result from errors in the Galactic diffuse model, some higher flux, nonvariable, unidentified sources are likely to be Galactic pulsars. The excess of variable, unidentified sources at low latitudes suggests that either pulsars can produce variable gamma rays under special circumstances, or that a new class of Galactic gamma-ray sources exists.

Subject headings: BL Lacertae objects: general — gamma rays: observations — quasars: general — radiation mechanisms: nonthermal

1. INTRODUCTION

In this paper, a method to calculate the mean fluxes and flux variabilities of high-energy gamma-ray sources is presented. The data consist of 128 sources listed in the second catalog of sources detected with the Energetic Gamma Ray Experiment Telescope (EGRET) (Thompson et al. 1995). These sources include the Large Magellanic Cloud, five pulsars, 39 active galactic nuclei (AGNs) identified with high confidence, 11 AGNs identified with lower confidence, and 72 sources not yet identified with known objects. Mattox et al. (1996a) find only two of the lower confidence AGN identifications to be compelling. We therefore include these two in the AGN category and treat the remaining nine as unidentified sources.

Comparisons among the variabilities of these different classes of sources will be made. In addition, the space distributions of variable and nonvariable sources will be examined. A table of mean fluxes and flux variabilities of all sources is included.

2. THE DATA

EGRET is the high-energy instrument on board the *Compton Gamma Ray Observatory* (*CGRO*). The instrument and its calibration are described by Thompson et al. (1993). The observations used for this project consist of the 134 viewing periods spanning the interval from 1991 April 22 to 1994 October 4 (phases 1, 2, and 3 of the *CGRO* mission). These viewing periods range from a few days to three weeks in length. Our analysis used binned maps of exposure and detected photons. The photon maps, binned into pixels of width 0°.5, include all events with estimated energies greater than 100 MeV.

3. FLUX CALCULATION AND VARIABILITY ANALYSIS

We have obtained flux estimates with likelihood analysis, the primary method of EGRET data analysis (Mattox et al. 1996b). This method simultaneously estimates the strength of the Galactic and isotropic diffuse emission, and that of a point source distributed as the EGRET point-spread function. We have used the standard 15° radius of analysis. The flux (in $\mathrm{cm}^{-2}\ \mathrm{s}^{-1}$) is calculated by dividing the counts estimate by the exposure. To obtain estimates of the probability of variability, we have extended the analysis of Thompson et al. (1995) in several ways. We have derived flux estimates for all sources for all viewing periods (instead of the 2 σ upper limits provided by Thompson et al. 1995 if the detection is less than 3 σ). In addition, Mattox et al. (1996b) point out that the flux estimate range is asymmetric about the flux estimate for small source counts. Because we expect that it improves the reliability of our variability analysis, we derive an upper and a lower flux estimate standard deviation, σ_+ and σ_-; σ_+ is the 68% counts upper limit minus the counts estimate. Similarly, σ_- is calculated as the estimate minus the 68% lower limit. In the case that statistical fluctuations result in a negative counts estimate, both the flux and σ_- are taken to be zero. In addition, if σ_+ is lower than the expected sensitivity for a 1 σ detection, it is set equal to this sensitivity to avoid unrealistically small upper limits. Figure 1 illustrates the flux variabilities of several typical EGRET sources, along with error bars.

A weighted mean flux, $\bar{F}$, is calculated as

$$\bar{F} = \left[\sum_{i=1}^{N_{\rm vp}} \frac{F(i)}{\sigma^2(i)}\right]\left[\sum_{i=1}^{N_{\rm vp}} \frac{1}{\sigma^2(i)}\right]^{-1}, \quad (1)$$

where $N_{\rm vp}$ is the number of viewing periods in which the source was observed. The deviation $\sigma(i)$ is taken to be the average of $\sigma_+(i)$ and $\sigma_-(i)$. In those cases in which $\sigma_-(i)$ equals zero, $\sigma(i)$ is set equal to $\sigma_+(i)$. The variance of the weighted mean flux is

$$\sigma_{\bar{F}}^2 = \left[\sum_{i=1}^{N_{\rm vp}} \frac{1}{\sigma^2(i)}\right]^{-1}. \quad (2)$$

To quantify the flux variability of a source, we calculate

$$\chi^2 = \sum_{i=1}^{N_{\rm vp}} \left[\frac{F(i) - \bar{F}}{\sigma(i)}\right]^2. \quad (3)$$

[1] Astronomy Department, Cornell University, Ithaca, NY 14850.
[2] Astronomy Department, University of Maryland, College Park, MD 20742.
[3] Space Astronomy Program, Universities Space Research Association.
[4] Code 661, Laboratory for High Energy Astrophysics, NASA Goddard Space Flight Center, Greenbelt, MD 20771.

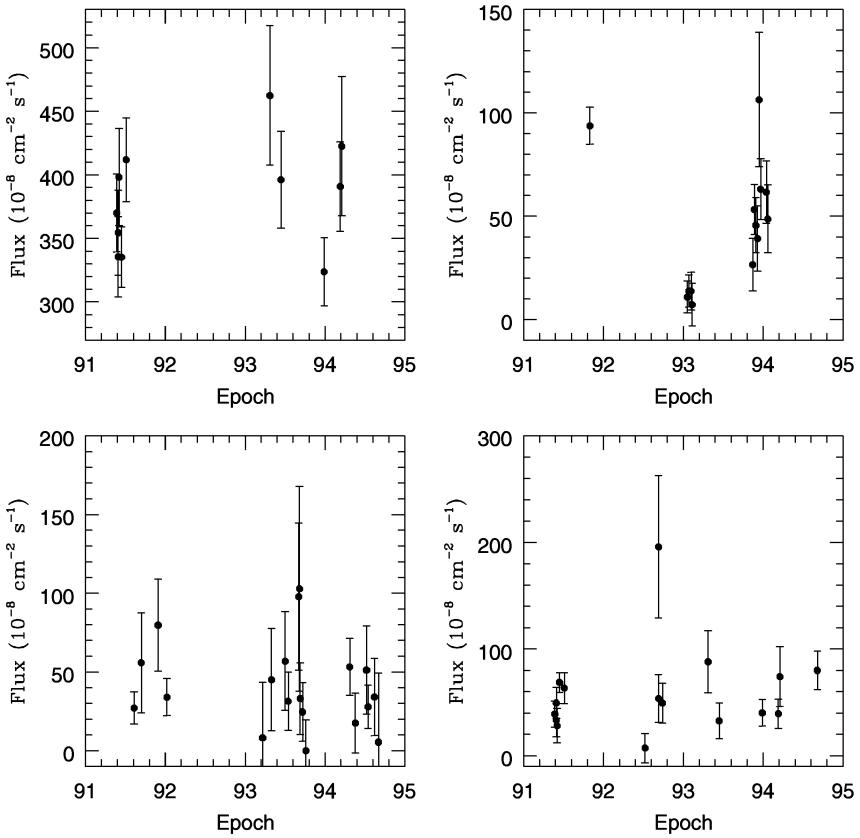

FIG. 1.—Flux variations, with error bars, for four EGRET sources over a ~3.5 yr time span. Typical flux variations for (*clockwise from upper left*) a pulsar (Geminga), an AGN (3C 279), a variable, unidentified source (2EG J0618+2234), and a nonvariable, unidentified source (2EG J1742−2250) are shown.

For a nonvariable source, the mean value of the χ^2 distribution is expected to be $N_{vp} - 1$, the number of degrees of freedom in our data. To determine whether the χ^2 value for a source suggests flux variability, we find the probability that a χ^2 value greater than the empirical χ^2 [i.e., $P(\chi^2 > \chi^2_{\rm empirical})$] could occur by chance for an intrinsically nonvariable source. This probability, Q, equals (Press et al. 1992)

$$Q = 1 - P\left(\frac{N_{vp} - 1}{2}, \frac{\chi^2}{2}\right), \quad (4)$$

where $P(a, x)$, $a \geq 0$, is the incomplete gamma function. For intrinsically nonvariable sources, the distribution of Q is uniform between 0 and 1.

Thompson et al. (1995) recommend that an additional flux uncertainty of 10% be added to the statistical uncertainty because of systematic error. They mention uncertainty in the instrumental calibration as a function of energy, angle within the instrument, and time as the performance of EGRET degrades as the gas ages. We use the most recent estimates of relative EGRET performance for each viewing period (Sreekumar et al. 1996) which differ by as much as ~10% from those used by Thompson et al. (1995). Additional systematic flux error could result from error in the Galactic diffuse model and from source confusion.

Because an accurate determination of the amount of systematic error is impractical, we cannot determine the absolute variability of sources. Therefore, we quantify the relative variability of sources by assuming the Galactic pulsars to be a nonvariable source population. We find that the distribution of pulsar χ^2 values is consistent with nonvariability if we include a systematic error of 6.5% ± 1.0%. We therefore calculate all source fluxes by adding this error in quadrature to both σ_+ and σ_-.

We define the variability index, $V = -\log Q$, to indicate the strength of the evidence for flux variability. A larger V corresponds to stronger evidence for variability. We classify sources as nonvariable if $V < 0.5$, uncertain if $0.5 \leq V < 1$, or variable if $V \geq 1$.

4. RESULTS FOR EGRET SOURCES

Table 1 lists the results for the 128 sources from the Second EGRET Catalog included in this study. The key to the table is as follows:

Column (*1*).—Source name, based on J2000 coordinates.
Column (*2*), (*3*)—Galactic longitude l and latitude b (in degrees) measured by EGRET.
Column (*4*).—Significance S of the EGRET detection in standard deviations [$(TS)^{1/2}$ from the likelihood analysis (Mattox et al. 1996b)], as given in Second EGRET Catalog.
Column (*5*).—Mean flux $\bar{F}$ (10^{-8} cm^{-2} s^{-1}), $E > 100$ MeV.
Column (*6*).— Standard deviation $\sigma_{\bar{F}}$ of the mean flux.
Column (*7*).—Deviation χ^2 of flux from the mean (eq. [3]).
Column (*8*).—Number of viewing periods N_{vp} in which the source was observed.
Column (*9*).—Variability index V ($V = -\log Q$, where Q is the significance of variability; a larger V corresponds to stronger evidence for variability).
Column (*10*).—Type of source: "P" = pulsar (indicates detection of pulsed gamma radiation); "G" = galaxy (the

TABLE 1

FLUX VARIABILITY OF EGRET SOURCES

Name	l	b	S	$\bar{F}$	$\sigma_{\bar{F}}$	χ^2	N_{vp}	V	Identification	Other Name
2EG J0000+2041.....	107.10	−40.60	4.7	10.9	3.5	7.6	6	0.75	A	2356+196
2EG J0008+7307.....	119.77	10.52	8.7	40.1	7.1	5.9	3	1.28		
2EG J0119+0312.....	136.77	−58.90	4.5	6.4	3.1	8.3	5	1.09		
2EG J0129−1748.....	168.21	−77.18	4.6	11.5	3.7	0.73	3	0.16		
2EG J0159−3557.....	248.55	−73.08	4.3	11.5	3.7	0.84	3	0.18		
2EG J0204+1512.....	147.72	−44.13	5.3	8.0	3.0	13.7	4	2.47	A	0202+149
2EG J0210−5051.....	276.10	−61.78	23.6	75.3	5.5	34.9	8	4.94	A	0208−512
2EG J0216+1107.....	153.93	−46.60	4.1	6.2	3.1	7.2	2	2.15		
2EG J0220+4228.....	139.88	−17.46	5.4	18.3	3.1	2.2	5	0.15		0219+428
2EG J0238+1657.....	156.51	−38.84	13.0	20.2	3.6	40.8	3	8.86	A	0235+164
2EG J0239+2818.....	150.18	−28.77	5.2	13.8	3.0	2.0	6	0.07	A	
2EG J0241+6119.....	135.74	1.22	14.6	88.2	7.7	13.5	6	1.72		
2EG J0323+5126.....	145.53	−4.65	5.0	14.7	3.9	8.1	7	0.64		
2EG J0403+3357.....	162.40	−13.79	4.5	6.9	2.6	11.9	12	0.43		
2EG J0406+1704.....	175.61	−25.23	4.0	6.7	2.8	12.4	16	0.19		
2EG J0422+1414.....	180.65	−24.26	6.0	14.3	3.1	14.7	16	0.33		
2EG J0423−0058.....	195.01	−32.80	6.7	15.0	3.7	18.6	10	1.54	A	0420−014
2EG J0426+6618.....	142.24	11.87	4.5	12.6	3.7	11.0	8	0.86		
2EG J0432+2910.....	170.34	−12.68	4.8	14.0	2.9	11.7	16	0.15		
2EG J0437+1524.....	182.10	−20.68	4.1	9.9	2.9	17.4	16	0.53		
2EG J0450+1122.....	187.58	−20.49	7.7	15.3	2.8	28.5	15	1.91	A	0446+112
2EG J0458−0122.....	200.53	−25.53	4.4	11.9	3.3	12.4	10	0.72	A	
2EG J0506+3424.....	170.85	−3.79	5.7	10.5	2.9	18.1	17	0.50		
2EG J0511+5523.....	154.40	9.35	5.0	19.0	3.6	3.8	8	0.09		
2EG J0520+2626.....	179.04	−6.07	6.3	17.0	3.0	14.6	17	0.26		
2EG J0521+2206.....	182.87	−8.18	6.2	17.1	3.4	18.5	16	0.63		
2EG J0524−3630.....	240.70	−32.52	4.7	13.6	3.5	12.0	4	2.12	A	0521−365
2EG J0531+1324.....	191.37	−11.01	26.1	58.0	3.8	145.7	15	23.29	A	0528+134
2EG J0532−6914.....	279.70	−32.16	6.6	13.4	2.5	14.2	8	1.32	G	LMC
2EG J0534+2158.....	184.56	−5.78	53.3	212.0	6.5	23.3	16	1.11	P	Crab PSR
2EG J0536−4348.....	249.70	−31.40	5.3	12.9	2.9	12.0	7	1.21	A	0537−441
2EG J0545+3943.....	170.79	5.65	5.4	12.8	2.8	13.7	17	0.21		
2EG J0617−0652.....	215.27	−10.62	5.1	11.5	4.1	9.7	9	0.54		
2EG J0618+2234.....	189.13	3.19	13.5	46.6	3.9	29.7	16	1.88		
2EG J0633+1745.....	195.13	4.27	80.9	367.1	10.4	12.4	11	0.59	P	Geminga
2EG J0635+0521.....	206.17	−0.99	5.1	20.2	4.2	9.0	14	0.11		
2EG J0720+7126.....	143.87	27.89	8.7	14.8	2.2	7.9	8	0.47	A	0716+714
2EG J0720−4746.....	259.24	−15.19	4.9	7.7	2.8	11.0	10	0.56		
2EG J0737+1725.....	202.09	17.91	4.0	14.5	3.5	7.1	10	0.20	A	0735+178
2EG J0744+5438.....	163.18	29.34	7.2	8.6	2.3	23.0	8	2.77		
2EG J0807+4849.....	170.37	32.28	4.6	11.4	2.6	3.6	9	0.05		
2EG J0809+5117.....	167.46	32.74	4.2	6.9	2.3	6.2	9	0.20		
2EG J0812−0648.....	228.64	14.55	5.7	21.7	5.4	4.0	4	0.59		
2EG J0828+0510.....	219.59	23.87	4.1	10.8	5.5	1.5	3	0.33	A	0829+046
2EG J0831+2403.....	200.20	31.91	5.3	18.8	4.1	2.4	4	0.31	A	0827+243
2EG J0831+7044.....	143.99	33.66	6.1	7.4	1.8	20.6	9	2.08	A	0836+710
2EG J0835−4513.....	263.55	−2.79	2.1	940.9	41.4	0.23	4	0.01	P	Vela PSR
2EG J0852−1237.....	239.35	19.75	5.0	7.4	3.7	10.9	4	1.91		
2EG J0917+4420.....	176.27	44.19	6.5	13.5	2.3	8.2	9	0.38		
2EG J0957+5515.....	158.81	47.91	4.7	7.0	1.5	16.5	13	0.77	A	0954+556
2EG J0958+6537.....	145.73	43.03	6.1	5.7	1.7	17.4	10	1.37	A	0954+658
2EG J1021−5835.....	284.45	−1.20	11.5	105.4	8.3	14.0	10	0.91		
2EG J1049−5847.....	287.58	0.58	7.7	61.3	7.6	6.3	11	0.10		
2EG J1054+5736.....	148.80	53.26	4.0	4.0	1.5	9.3	13	0.17		
2EG J1059−5237.....	285.98	6.65	7.0	23.6	3.5	5.4	12	0.04	P	PSR 1055−52
2EG J1103−6106.....	290.30	−0.90	6.9	47.3	7.6	10.2	11	0.38		
2EG J1104+3812.....	179.83	65.03	8.5	13.9	2.0	7.4	8	0.41	A	MRK 421
2EG J1134−1515.....	276.84	43.71	6.0	6.5	2.5	26.8	13	2.08	A	1127−145
2EG J1136−0414.....	270.26	53.84	4.1	4.7	2.0	13.1	15	0.28		
2EG J1158+2906.....	200.18	78.21	7.0	4.2	1.8	15.8	13	0.70	A	1156+295
2EG J1224+2155.....	251.83	81.96	8.2	12.6	1.9	39.9	18	2.88	A	1222+216
2EG J1229+0206.....	289.95	64.36	7.4	17.9	2.1	24.7	13	1.79	A	3C 273
2EG J1230−0254.....	292.78	59.57	5.0	7.9	1.8	10.6	13	0.25	A	1229−021
2EG J1233−1407.....	296.20	48.50	4.9	6.0	2.1	13.6	17	0.20		
2EG J1239+0441.....	295.04	67.38	6.3	9.1	1.8	9.2	13	0.16		
2EG J1248−8308.....	302.83	−20.27	4.9	12.9	3.5	11.8	7	1.18		
2EG J1256−0546.....	305.10	57.06	42.7	30.3	3.0	81.6	13	11.69	A	3C 279
2EG J1314+5151.....	114.42	64.88	4.0	7.4	2.2	3.8	6	0.23		
2EG J1314−3430.....	308.39	28.11	7.7	16.8	2.9	5.9	8	0.26		
2EG J1324−4317.....	309.32	19.16	6.3	16.1	2.9	8.1	11	0.21		
2EG J1330+1652.....	346.02	76.39	4.0	6.3	2.1	6.0	15	0.02	A	1331+170
2EG J1332+8821.....	122.60	28.75	4.0	9.4	2.4	5.7	7	0.34		
2EG J1346+2942.....	48.11	77.57	4.4	7.6	3.2	6.5	9	0.23		
2EG J1409−0742.....	333.88	50.28	16.0	18.0	3.3	96.3	10	16.06	A	1406−076
2EG J1412−6211.....	312.28	−0.81	7.4	71.8	9.8	8.7	11	0.25		

TABLE 1—*Continued*

Name	l	b	S	$\bar{F}$	$\sigma_{\bar{F}}$	χ^2	N_{vp}	V	Identification	Other Name
2EG J1430+5356.....	95.52	57.58	4.1	2.3	2.5	6.6	7	0.45		
2EG J1443−6040.....	316.28	−0.75	5.2	42.6	9.3	14.6	10	0.99		
2EG J1457−1916.....	339.68	34.46	4.0	9.2	3.6	10.4	7	0.96		
2EG J1513−0857.....	351.47	40.21	4.9	15.6	4.2	9.4	5	1.29	A	1510−089
2EG J1528−2352.....	343.23	26.45	4.6	6.4	3.2	16.4	13	0.76		
2EG J1605+1558.....	29.25	43.92	4.9	11.6	4.1	8.8	6	0.93	A	1604+159
2EG J1608+1046.....	23.35	40.94	7.8	16.0	4.3	22.2	6	3.32	A	1606+106
2EG J1614+3431.....	55.62	46.22	7.9	12.5	3.6	24.4	4	4.68	A	1611+343
2EG J1626−2452.....	352.68	16.63	7.8	30.5	4.0	15.8	15	0.49	A	
2EG J1631−2845.....	350.40	13.26	6.0	17.1	3.5	18.9	15	0.77		
2EG J1635+3813.....	61.09	42.34	17.1	53.2	5.9	27.3	4	5.30	A	1633+382
2EG J1635−1427.....	2.57	21.67	4.1	10.5	3.1	8.2	16	0.04		
2EG J1648−5042.....	335.95	−3.68	5.5	36.1	7.1	10.1	13	0.22		
2EG J1709−0350.....	17.07	20.63	4.0	10.8	3.9	6.9	13	0.06		
2EG J1710−4432.....	343.10	−2.69	18.8	118.7	7.2	12.9	17	0.17	P	PSR 1706−44
2EG J1718−3310.....	353.31	2.48	5.0	26.9	6.1	18.2	17	0.50		
2EG J1731+6007.....	88.93	33.14	4.2	8.1	3.3	7.4	9	0.31		
2EG J1735−1312.....	12.20	10.30	7.1	25.4	3.5	31.3	19	1.58	A	1730−130
2EG J1739+5152.....	79.17	31.95	7.4	19.6	3.7	13.0	9	0.95	A	1739+522
2EG J1742−2250.....	4.78	3.86	6.8	31.8	4.6	13.5	19	0.12		
2EG J1746−0935.....	16.76	9.81	5.5	17.2	3.8	12.8	18	0.12		
2EG J1746−2852.....	0.17	−0.15	12.7	123.8	8.3	31.8	20	1.49		
2EG J1747−3039.....	358.77	−1.30	5.2	38.7	7.0	19.4	20	0.37		
2EG J1801−2312.....	6.73	−0.14	6.6	59.9	7.2	11.2	19	0.05		
2EG J1811−2339.....	7.52	−2.47	5.4	32.0	5.7	32.3	19	1.69		
2EG J1813−1229.....	17.52	2.53	7.3	47.7	6.3	41.1	18	3.05		
2EG J1815+2950.....	56.89	20.37	4.0	7.1	2.7	11.0	13	0.27		
2EG J1821−7915.....	314.72	−25.25	6.1	26.8	5.8	3.9	7	0.17		
2EG J1825−1307.....	18.38	−0.43	6.7	69.0	7.8	28.6	18	1.41		
2EG J1828+0145.....	31.92	5.82	6.5	13.8	6.0	24.6	10	2.46		
2EG J1834−2138.....	11.77	−6.22	5.2	20.3	3.6	21.6	20	0.52		
2EG J1835+5919.....	88.74	25.12	18.1	58.9	4.6	18.3	11	1.30		
2EG J1847−3220.....	3.17	−13.33	4.2	8.0	2.6	15.0	19	0.18		
2EG J1850−2638.....	8.82	−11.70	4.0	9.2	2.8	15.9	19	0.22		
2EG J1857+0118.....	34.80	−0.76	5.1	58.6	9.4	14.6	9	1.17		
2EG J1911−1945.....	17.28	−13.22	5.4	16.1	2.8	12.0	19	0.07	A	1908−201
2EG J1934−4014.....	358.73	−24.96	4.8	9.8	3.0	21.5	12	1.54	A	1933−400
2EG J1950−3503.....	5.17	−26.50	5.5	7.4	3.0	17.1	12	0.97		
2EG J2006−2253.....	19.32	−26.17	4.1	5.8	2.8	17.3	11	1.17		
2EG J2019+3719.....	75.46	0.60	11.5	75.7	6.5	22.4	13	1.48		
2EG J2020+4026.....	78.12	2.23	17.5	114.9	7.3	16.9	13	0.81		
2EG J2023−0836.....	35.68	−24.43	7.8	16.1	3.6	24.6	6	3.78		
2EG J2026+3610.....	75.31	−1.18	7.1	38.6	5.8	20.1	13	1.19		
2EG J2027+1054.....	54.24	−15.55	4.4	4.1	2.9	11.1	13	0.28		
2EG J2033+4112.....	80.19	0.66	10.6	69.0	6.9	16.1	14	0.61		
2EG J2039+1131.....	56.46	−17.71	4.4	10.3	3.0	12.7	11	0.62		
2EG J2058−4657.....	352.95	−40.70	4.2	7.2	3.3	8.5	4	1.43	A	2052−474
2EG J2210+2358.....	81.87	−25.75	4.1	6.1	3.0	7.9	10	0.27	A	2209+236
2EG J2227+6122.....	106.60	3.14	7.0	46.7	7.1	6.0	7	0.38		
2EG J2233+1140.....	77.58	−38.76	8.1	22.0	3.5	8.3	7	0.67	A	CTA 102
2EG J2243+1545.....	83.17	−37.04	4.0	6.8	3.5	10.3	7	0.95		
2EG J2253+1615.....	86.11	−38.18	16.7	63.1	5.3	19.5	7	2.46	A	3C 454.3
2EG J2354+3811.....	110.73	−23.32	4.6	6.4	3.7	10.0	5	1.40		

Large Magellanic Cloud is the only one in this sample); "A" = active galactic nucleus.

Column (*11*).—Name of the identified source from the Second EGRET Catalog.

The mean fluxes and standard deviations in Table 1 differ slightly from those given in the Second EGRET Catalog for several reasons. We have used a revised EGRET data set (Sreekumar et al. 1996) which includes energy-dependent corrections for the instrument performance as a function of time. In addition, more viewing periods were included in our flux calculations. Finally, as described in § 3, a 6.5% systematic error was added in quadrature to the statistical flux errors.

Because the calibration of the sensitivity of EGRET is less accurate at large angles from the instrument axis, we only include viewing periods in which the source is within 29 degrees of the instrument axis in this analysis. (The sensitivity has decreased to roughly 15% of on-axis sensitivity at this angle.) No correlation is found between the number of nearby sources and the detected variability of a source. In addition, no significant correlation between the exposure time per viewing period and the detected variability of a source was found.

4.1. *Variability Distributions*

Figure 2 shows the distribution of V for all sources. Of the 128 sources, 55 are found to be nonvariable ($V < 0.5$),

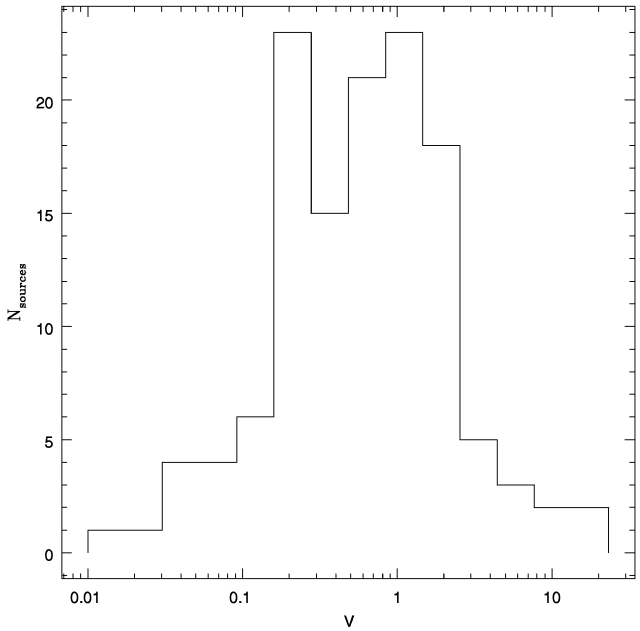

FIG. 2.—Histogram of V for all sources

28 have uncertain variability ($0.5 \leq V < 1$), and 45 are found to be variable ($V \geq 1$). These cutoffs were chosen to obtain similar numbers of sources in each group and to minimize both type 1 and type 2 errors. The $V \geq 1$ variability criterion corresponds to $Q \leq 0.1$. Because the Q values of intrinsically nonvariable sources are distributed uniformly between 0 and 1, 10% of the intrinsically nonvariable sources will incorrectly be classified as variable. However, a more stringent cutoff would result in missing many of the intrinsically variable sources. The criterion for nonvariability of $V < 0.5$ corresponds to $Q > 0.3$. Therefore, 30% of the intrinsically nonvariable sources will be excluded from the nonvariable source group, but contamination from intrinsically variable sources will be small. (We cannot estimate the extent of this in detail because the Q distribution is unknown.) While the above criteria for variability/nonvariability are somewhat arbitrary, changing these criteria by up to $\pm 20\%$ yields similar results.

The 55 sources in the nonvariable group include three pulsars, 11 AGNs, and 41 unidentified sources. The 45 variable sources include the LMC, the Crab pulsar,[5] 23 AGNs, and 20 unidentified sources. The 28 sources not included in either variable or nonvariable groups include one pulsar, seven AGNs, and 20 unidentified sources. Of the 10 most strongly variable ($V > 3$) sources, eight are AGNs and two have not been identified with any known sources. Figure 3 shows the V distributions of AGNs, pulsars, and unidentified sources.

All four of the identified AGNs with an average flux $\bar{F} > 40 \times 10^{-8}$ cm^{-2} s^{-1} are variable. Of the weaker flux sources identified with AGNs, only 50% are found to be variable. However, because our methods are not as sensitive to variability in lower flux sources, it is possible that the

[5] The Crab pulsar's variability index of $V = 1.11$ is not strongly indicative of variability. Moreover, because variability has been detected in the unpulsed Crab emission (DeJager et al. 1996), the Crab's variability is most likely due to the surrounding nebula and is not intrinsic to the pulsar.

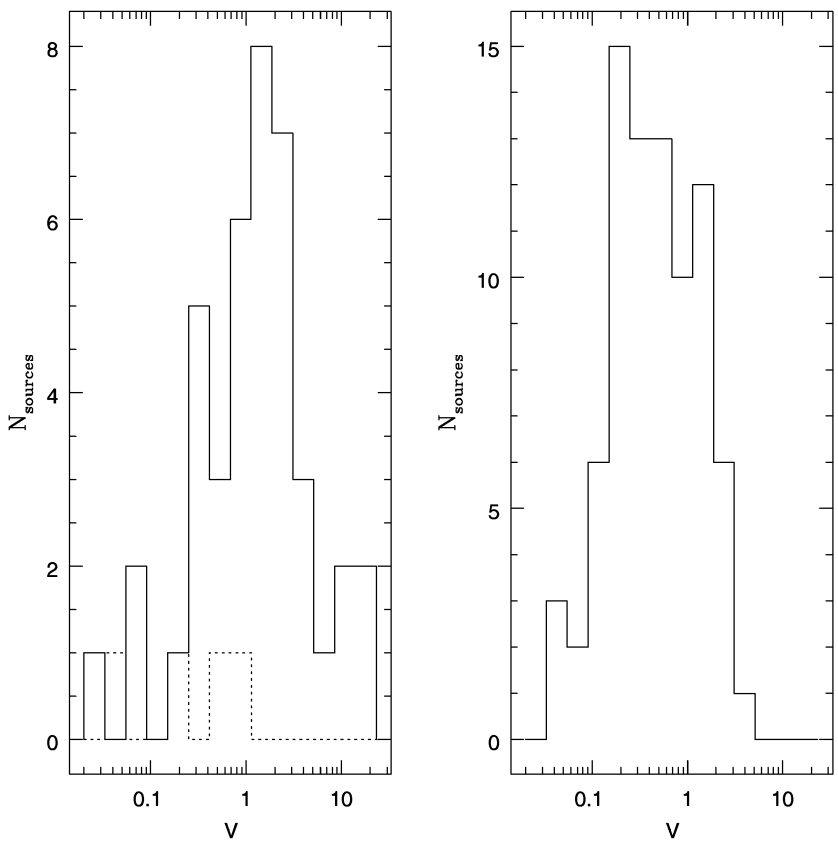

FIG. 3.—*Left: V* distributions for identified AGNs (*solid line*) and identified pulsars (*dotted line*) are shown. *Right: V* distribution for unidentified sources. The x-axis scales of the figures are identical.

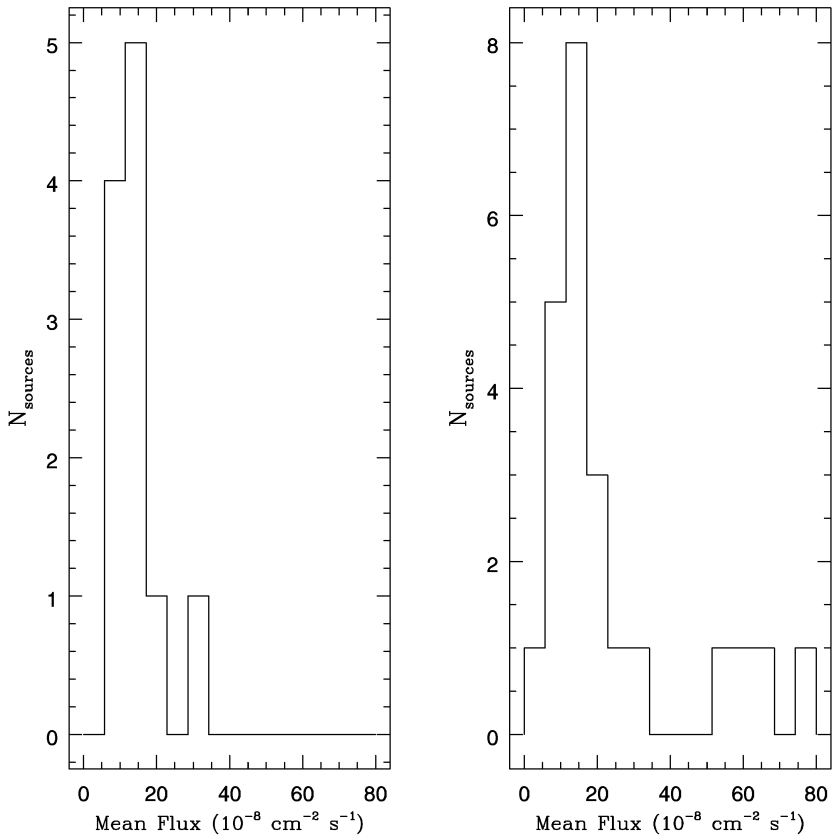

FIG. 4.—*Left:* mean flux distribution for nonvariable AGNs. *Right:* mean flux distribution for variable AGNs. The *x*-axis scales of the figures are identical.

gamma-ray emission of all AGNs is intrinsically variable. This dependence of detected variability upon source flux is easily seen by expressing a source's χ^2 value as

$$\chi^2 = \sum_{i=1}^{N_{\rm vp}} \epsilon^2(i)\left[\frac{\bar{F}}{\sigma(i)}\right]^2, \qquad (5)$$

where $\epsilon(i)$, defined as $[F(i) - \bar{F}]/\bar{F}$, is the percentage by which a source's flux varies from the mean in viewing period i. Equation (5) shows that a source's χ^2 value, and hence its variability index V, is reduced if the ratio of its mean flux to its standard deviation is small. Assuming Poisson statistics, this ratio will be lower for lower flux sources. The ratio will also be decreased at low latitudes, where the Galactic diffuse emission is higher.

Figure 4 shows that, while there is some overlap in the mean flux distributions of variable and nonvariable AGNs, there are no nonvariable, high-flux AGNs. Furthermore, Figure 5 demonstrates that nonvariable AGNs are more concentrated toward lower latitudes than are variable AGNs. Therefore, it is clear that some intrinsically variable AGNs are incorrectly classified as nonvariable because of decreased sensitivity to variability in low-flux sources and at low latitudes.

Similarly, Figure 6 shows the mean flux/variability relation for unidentified sources. While, in general, more variability is found in higher flux sources, the existence of *several nonvariable sources with high fluxes implies a genuine population of nonvariable, unidentified sources.*

4.2. *Latitude Distributions*

We find that the latitude distributions of variable and nonvariable sources differ. Figure 7 compares the cumulative distribution function (cdf) of each subset with the theoretical cdf of a source population distributed uniformly in sin b ($-90° < b < 90°$). Using the Kolmogorov-Smirnoff test (Press et al. 1992), we calculate a 28% probability that the variable source distribution is drawn from an isotropically distributed source population. For nonvariable

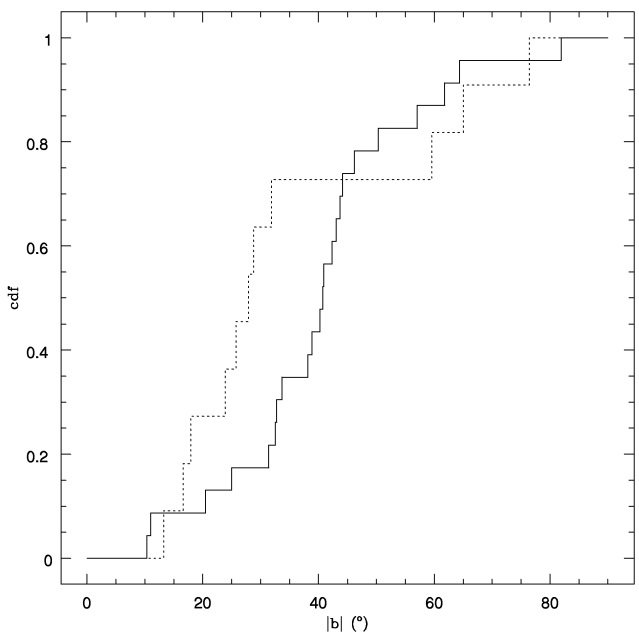

FIG. 5.—Comparison of cumulative distribution functions of nonvariable (*dotted line*) and variable (*solid line*) AGNs.

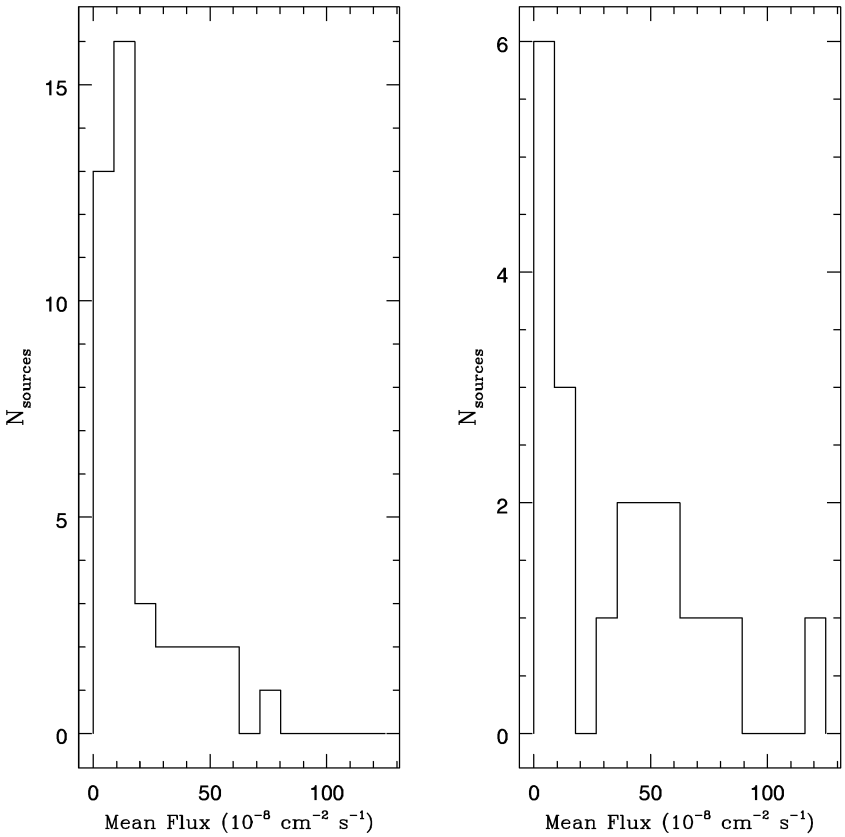

FIG. 6.—*Left:* mean flux distribution for nonvariable, unidentified sources. *Right:* distribution for variable, unidentified sources. The *x*-axis scales of the figures are identical.

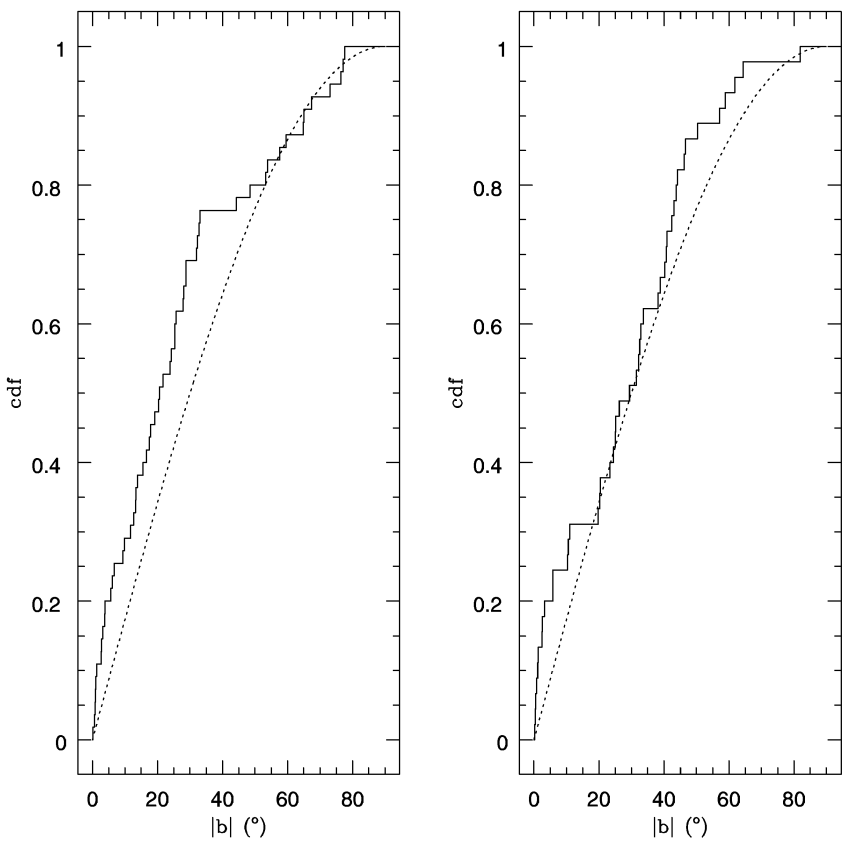

FIG. 7.—*Left:* comparison of the cumulative distribution function (cdf) of nonvariable sources (*solid line*) with that expected for an isotropic distribution (*dotted line*). *Right:* comparison of the cdf of the variable sources with that of an isotropic distribution.

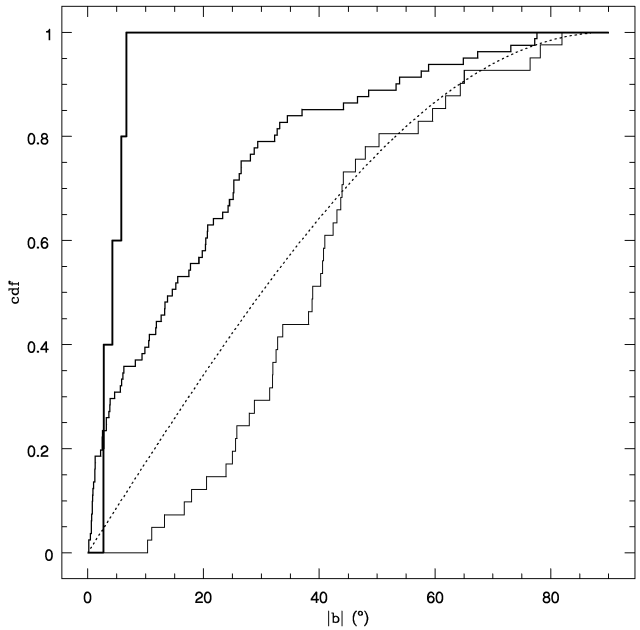

FIG. 8.—Comparison of the cdfs of three source populations: pulsars (*thickest line*), unidentified sources (*medium line*), and AGN (*thinnest line*). The dotted line denotes the cdf of an isotropic distribution.

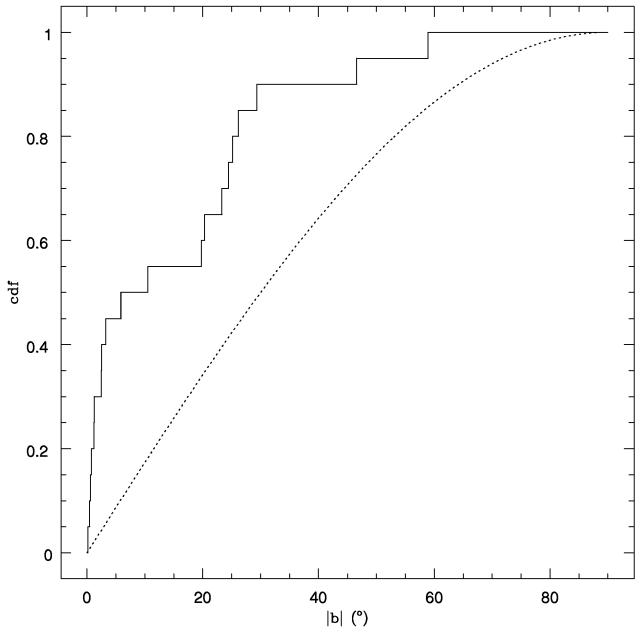

FIG. 10.—Cdf of variable, unidentified sources (*solid line*). The dotted line indicates the cdf of an isotropically distributed source population.

sources, the corresponding probability is 0.93%. Figure 7 shows that, while the variable sources appear to be distributed approximately isotropically, nonvariable sources are concentrated toward lower latitudes.

In Figure 8 the cdfs of the different source populations are compared. The latitude distributions of the three types of identified sources differ significantly. All pulsars are in the plane of the Galaxy, identified AGNs are concentrated toward higher latitudes, and unidentified sources are concentrated toward lower latitudes.

The apparent anisotropy of the AGN cdf can be explained by the decreased sensitivity of EGRET at low latitudes. Mattox et al. (1996b) find that EGRET's minimum detectable flux, $F_{\rm min}$, is adequately represented by

$$F_{\rm min} \propto S\sqrt{\frac{B}{E}}\ , \qquad (6)$$

where S is the significance of the detection in standard deviations, B is the background flux, and E is the exposure. The minimum detectable flux is higher at low latitudes because

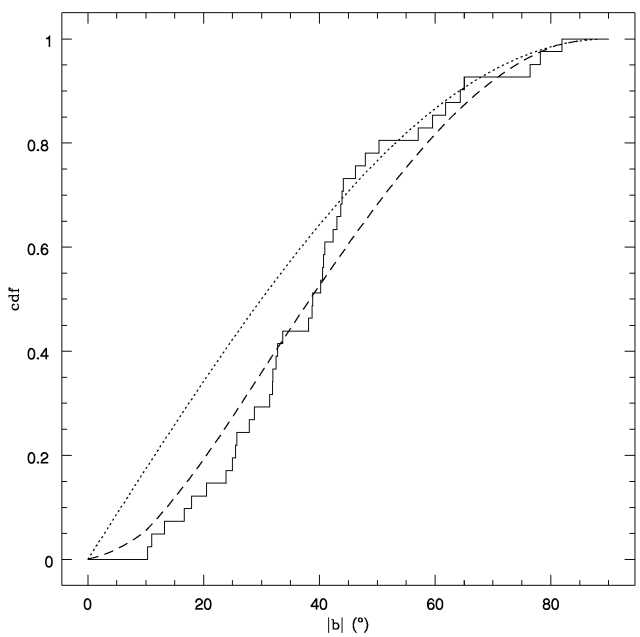

FIG. 9.—Cdf of identified AGN (*solid line*), the cdf of the modeled distribution of eq. (7) (*dashed line*), and the cdf of an isotropic source distribution (*dotted line*).

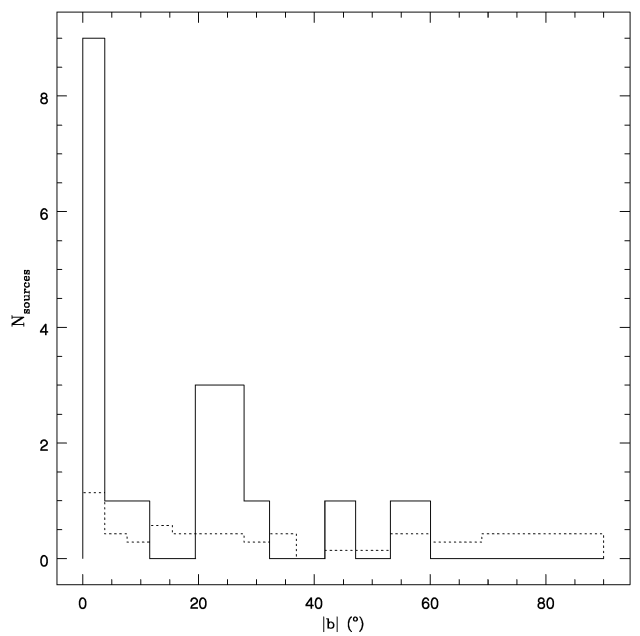

FIG. 11.—Solid line shows the $|b|$ distribution of the unidentified, variable sources. The dotted line indicates the distribution of nonvariable, unidentified sources that are expected to be incorrectly classified as variable. All histogram bins contain equal solid angle.

both the background flux and the minimum significance required for detection (used in the Second EGRET Catalog) are higher. Assuming that AGNs are distributed isotropically, the number of identified AGNs per steradian with fluxes greater than the minimum detectable flux will be proportional to $F_{\rm min}^{-3/2}$. We calculate the expected number per steradian of detected AGNs to be

$$\frac{dN}{d\Omega} = \frac{dN_{\rm high}}{d\Omega}\left(\frac{S}{S_{\rm high}}\right)^{-3/2}\left(\frac{B}{B_{\rm high}}\right)^{-3/4}. \quad (7)$$

In the above equation, $dN_{\rm high}/d\Omega$ is the number per steradian of identified AGNs at high latitudes ($dN_{\rm high}/d\Omega \approx 5.4$); $S_{\rm high}$ is the significance criterion required for detection at high latitudes ($S_{\rm high} = 4$); $B_{\rm high}$ is the background flux at high latitudes ($B_{\rm high} \approx 2 \times 10^{-5}$ cm^{-2} s^{-1} sr^{-1}). Equal exposures at high and low latitudes are assumed. By estimating the background flux at a specific latitude and accounting for the higher significance criterion of $S = 5$ at $b < 10°$, we can model the expected latitude distribution of identified AGNs using equation (7). Figure 9 compares the cdf of this modeled distribution with the measured cdf of identified AGNs. Using the Kolmogorov-Smirnoff test, we calculate a 29% probability that identified AGNs are distributed according to our model. *We therefore conclude that the apparent paucity of AGNs at lower latitudes can be explained by the decreased sensitivity to sources at those latitudes.*

The anisotropy of the unidentified source cdf is more difficult to explain. Galactic diffuse model errors, which are not well quantified, could introduce some spurious, low-latitude, nonvariable sources. However, diffuse model error cannot explain the large excess of *variable*, unidentified sources at low latitudes (Fig. 10). A Kolmogorov-Smirnoff test yields a 0.15% probability that the variable, unidentified sources are drawn from an isotropic distribution. Because decreasing EGRET sensitivity at low latitudes sufficiently explains the distribution of identified AGNs, these excess variable sources are highly unlikely to be unidentified AGNs. We recall that some of these excess variable sources are intrinsically nonvariable sources that have been incorrectly classified as variable. Because of the variability criterion of $V \geq 1$, 10% of the intrinsically nonvariable sources will be incorrectly included in the variable source category. Figure 11 compares the distribution of variable, unidentified sources with that of the expected contaminating population (i.e., 10% of the unidentified, nonvariable sources plus an additional (10/7)% because of the $Q \geq 0.3$ nonvariability cutoff). This population can only account for 30% of the unidentified, variable sources. *Therefore, we conclude that these unidentified, low-latitude, variable sources represent an authentic source population.*

5. DISCUSSION AND CONCLUSIONS

We have developed a method for detecting flux variability and have applied it to 128 sources from the Second EGRET Catalog. Figure 12, an Aitoff plot of all sources, summarizes our results. We find that all identified Galactic pulsars are consistent with being nonvariable. All high-flux, identified AGNs and many low-flux, identified AGNs are variable. The apparent nonvariability of the remaining AGNs owes at least partly to decreased sensitivity to flux variability in low-flux and low-latitude sources.

We recognize populations of nonvariable and variable unidentified sources, both of which are in excess at low Galactic latitudes. Because of the uncertainty of the Galactic diffuse model at low latitudes, many low-flux, nonvariable, unidentified sources may result from diffuse model errors. However, higher flux, nonvariable, unidentified sources at low latitudes represent a definite source population and are excellent Galactic pulsar candidates.

While an uncertain Galactic diffuse model could produce spurious nonvariable sources, it is not expected to result in an excess of variable, unidentified sources at low latitudes. Because decreased EGRET sensitivity at low latitudes sufficiently explains the distribution of identified AGNs, these excess variable, unidentified sources are unlikely to be AGNs. Furthermore, the variability of these sources is inconsistent with the steadiness of the five known pulsars.

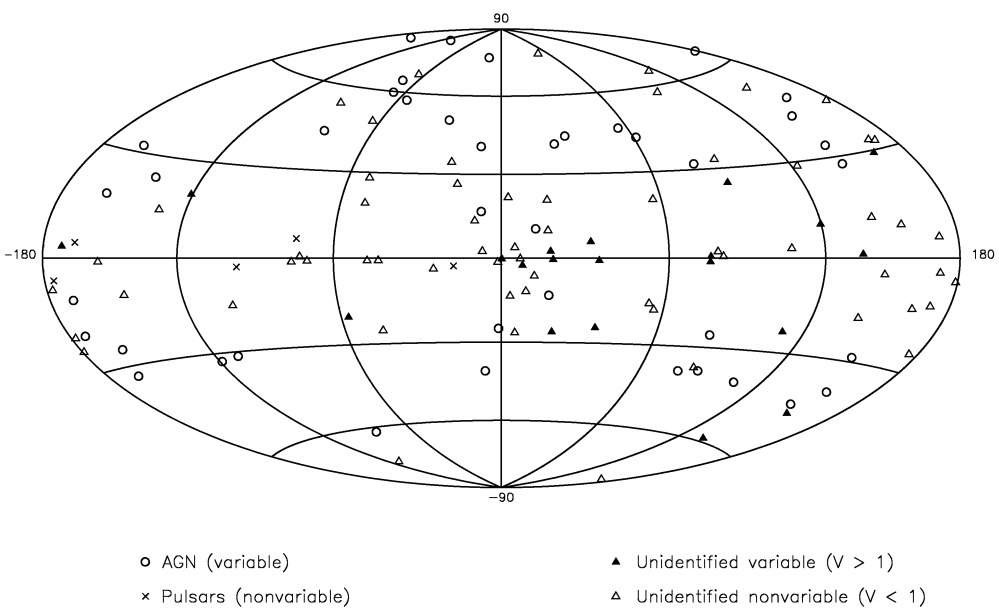

FIG. 12.—Aitoff projection illustrates the spatial distribution of all sources

Hence, these low-latitude, variable gamma-ray objects cannot be easily related to any known source population.

Several possible mechanisms could be responsible for such low-latitude, variable gamma-ray sources. They may represent active "hot spots" in the Galactic gamma-ray background caused by the interaction of energetic cosmic-ray particles with small-scale inhomogeneities in supernova remnants, molecular clouds, or star-forming regions in the Galactic plane. Kaaret & Cottem (1996) find 16 of the 25 unidentified EGRET sources with $b < 10°$ to be in or near OB associations, sites of massive star formation. We find seven of these 16 sources to be variable, suggesting that massive star formation and accompanying supernova phenomena, including interactions of young neutron stars with their very local environments, may lead to variable gamma rays. Alternatively, variable gamma-ray production could be caused by young, high-velocity pulsars interacting with clumps of gas in their paths. In addition, Tavani (1995) outlines a method for young pulsars in massive binary systems to produce unpulsed, variable gamma-ray emission through the shock interaction of their particle winds with circumbinary material. Such time-variable gamma-ray emission is consistent with multiwavelength observations of the 47 ms pulsar PSR 1259−63, which orbits a massive Be star (Tavani 1995). While PSR 1259−63 is not an EGRET source, Tavani suggests (Tavani et al. 1996) that this model may describe the time-variable, unidentified EGRET source 2EG J0241+6119. Tavani also shows how millisecond pulsars in low-mass binaries may be capable of variable gamma-ray emission through the interaction of their particle winds with the mass outflows from their irradiated companion stars. The pulsed radio emission from these millisecond pulsars may be undetectable as such pulsars are likely to be enshrouded in a cloud of evaporated companion material. Finally, the varying nebular particle acceleration (de Jager et al. 1996) most likely responsible for the slight variability of the Crab pulsar may result in stronger variability in similar young pulsars with denser surrounding remnants and/or lower pulsed fluxes. These two properties may have prohibited detection of pulsed radio emission from such objects thus far.

The appended table listing variabilities, mean fluxes, and positions of all unidentified sources can be referenced to choose sources for future study and observation at other wavelengths. Both Table 1 and a comprehensive table listing each source's flux, exposure, and aspect angle in all viewing periods are available at http://astrosun.tn.cornell.edu/SPIGOT/papers.html#gamma.

M. A. McL. acknowledges support from an NSF fellowship. J. R. M. acknowledges support from NASA Grants NAG5-2833 and NAGW-4761. This research was supported by NASA through GRO grant NAG5-2436 to Cornell University.

REFERENCES

de Jager, O. C., et al. 1996, ApJ, 457, 253
Kaaret, P., & Cottam, J. 1996, ApJ, 462, 35
Mattox, J. R., et al. 1996a, ApJ, 476, in press
———. 1996b, ApJ, 461, 396
Press, W. H., Teukolsky, S. A., Vetterling, W. T., & Flannery, B. P. 1992, Numerical Recipes: The Art of Scientific Computing (Cambridge: Cambridge Univ. Press)
Sreekumar, P., et al. 1996, in preparation
Tavani, M. 1995, in The Gamma Ray Sky with *Compton GRO* and SIGMA, ed. M. Signore, P. Salati, & G. Vedrenne (Dordrecht: Kluwer), 181
Tavani, M., et al. 1996, A&A, in press
Thompson, D. J., et al. 1993, ApJS, 86, 629
———. 1995, ApJS, 101, 259